Title: A computationally efficient thermomechanical model for the in-situ polymerization of a methyl methacrylate-based resin in a thick glass fiber laminate

Authors: Sarah F. Gayot[1,2]
Christian Bailly[2]
Thomas Pardoen[1]
Pierre Gérard[3]
Frederik Van Loock[1]

ABSTRACT

A computationally efficient thermochemical model is used to predict thermal runaway and the occurrence of monomer boiling during the in-situ polymerization of a methyl methacrylate (MMA)-based resin within a thick glass fiber layup. The framework couples the auto-accelerating exothermic free-radical bulk polymerization of MMA with the transfer of heat within the system and to the environment. Three approaches are considered for the kinetic treatment of the auto-acceleration: (1) an empirical model, (2) a semi-empirical model and (3) an analytical model. Predictions made via the three kinetic models are compared with experimental data measured during infusion tests with different processing conditions. Processing diagrams are constructed to reveal manufacturing regimes of interest for the production of thick fiber-reinforced methacrylic composites free of voids due to monomer boiling.

INTRODUCTION

Transitioning from thermosetting to thermoplastic resin matrices is the mainstream path followed by the composite community to enhance the recyclability of fiber-reinforced polymer composites. A dedicated range of methyl methacrylate (MMA)-based resins has recently been designed for the production of thermoplastic fiber-reinforced polymer composites via standard liquid molding processing routes [1]. The monomer-based resin is infused through a fibrous preform before undergoing in-situ polymerization.

[1]Institute of Mechanics, Materials & Civil Engineering, UCLouvain, Place Sainte-Barbe 2, 1348 Louvain-la-Neuve, Belgium
[2]Institute of Condensed Matter & Nanosciences, UCLouvain, Place Croix-du-Sud 2, 1348 Louvain-la-Neuve, Belgium,
[3]Groupement de Recherche de Lacq, Arkema, Route Départementale 817, BP 34, 64170 Lacq, France

However, producing thick (> 1cm) laminates with this resin system can be a practical challenge: the free-radical polymerization kinetics of MMA exhibits a 'gel effect' [2,3], i.e. the reaction auto-accelerates when the degree of monomer conversion exceeds a critical value. The temperature within the preform rises significantly, this thermal runaway may cause cavitation in the polymerizing matrix if the residual monomer starts to boil [1,4,5].

Manufacturing methods must be tailored to control the exothermic auto-accelerating behavior of MMA polymerization (i.e. to avoid monomer boiling) while still leading to short polymerization times. For this purpose, a few thermochemical models have been developed to predict the temperature field across the thickness of an MMA-based composite as a function of key processing parameters such as preform thickness [5–7]. These models give predictions by solving a heat transfer equation with an internal heat source term accounting for the heat released during polymerization. The recent one-dimensional model of Gayot et al. [7] is the first experimentally-validated thermochemical framework to account for the auto-accelerating exothermic nature of the polymerization reaction of MMA polymerization, known as the gel effect.

The gel effect is due to a reduction of the diffusivity of polymer radicals as the polymerization reaction proceeds. From a kinetic viewpoint, this corresponds to a decrease of the rate coefficient of radical termination k_t as monomer conversion χ increases [2,3]. Empirical models [8–11] as well as analytical models (based on free volume theory [12–17]) have been reported to predict the dependence of k_t on conversion. However, there is no consensus on the appropriate modelling strategy for the kinetic reaction of MMA within a thermochemical framework [5–7]. Calibrated empirical models may give more accurate predictions for sophisticated polymerization conditions (e.g. industrial reactors, multiple initiators and/or non-isothermal conditions) [10] but may only be suitable for these specific applications and not applicable to other experimental settings [18].

In this work, we make use of the recent model of Gayot et al. [7] to predict the maximum temperature during the polymerization of a MMA-based resin within a thick glass fiber layup. The thermochemical framework of Gayot et al. makes use of the analytical model of Achilias [15–17] to simulate the auto-accelerating nature of the polymerization of MMA. Here, we extend Gayot and co-workers' model [7] by considering an empirical and a semi-empirical approach to simulate the auto-accelerating kinetics of the reaction. Predicted temperature profiles via the three approaches (empirical, semi-empirical and analytical) are compared to measured temperature profiles for two infusion and in-situ polymerization tests with distinct mold heating conditions. The predictive capacity of the three (calibrated) versions of the thermochemical model is discussed. Processing maps are constructed to illustrate how the framework can be used to find optimal manufacturing conditions for thick glass fiber-reinforced methacrylic composites.

THERMOCHEMICAL MODEL

Theory

The one-dimensional thermochemical model by Gayot et al. [7] is used to predict the temperature T and degree of monomer conversion χ as a function of polymerization

time t across the thickness y of a glass fiber preform, see Fig. 1. The infused composite preform is idealized as a slab of homogeneous material with a uniform thermal diffusivity α_1. The dependence of T upon position coordinate y and time t is calculated by solving the following heat equation:

$$\frac{\mathrm{d}T}{\mathrm{d}t} = \alpha_1 \frac{\mathrm{d}^2T}{\mathrm{d}y^2} - \frac{\Delta H}{C_\mathrm{p} M_\mathrm{w}^0} \frac{\mathrm{d}M}{M_0 \mathrm{d}t} \quad , \tag{1}$$

where C_p is the temperature-dependent specific heat capacity of the composite, ΔH is the polymerization enthalpy, M_w^0 is the molecular weight of the MMA monomer, $\mathrm{d}M/\mathrm{d}t$ is the rate of change of the monomer concentration and M_0 is the initial monomer concentration.

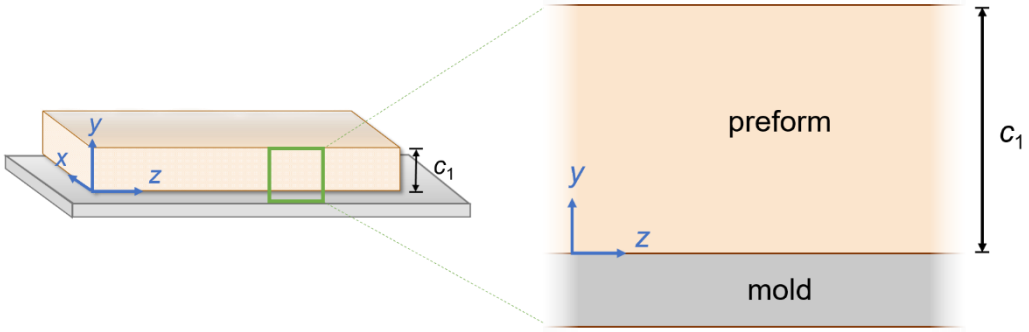

Figure 1: Coordinate system used for modelling the in-situ polymerization of an MMA-infused preform [7].

Five coupled kinetic equations governing the polymerization reaction of MMA are used to calculate the value of dM/dt; these are summarized in Table I. Several assumptions may be used to simplify this system of equations, namely the long-chain hypothesis, Flory's hypothesis and the quasi-steady state approximation (QSSA) for radical species [7,19]. Consequently, the rate of change of monomer concentration dM/dt reads:

$$\frac{\mathrm{d}M}{\mathrm{d}t} = -k_\mathrm{p} M \sqrt{\frac{r_\mathrm{i}}{k_\mathrm{t}}} = -k_\mathrm{p} M \sqrt{\frac{2 f k_\mathrm{d} I}{k_\mathrm{t}}} \quad , \tag{2}$$

where I is the initiator concentration, f is the efficiency factor of the initiator, and k_p, k_t and k_d are the temperature-dependent rate coefficients of the radical propagation, radical termination and initiator decomposition steps, respectively.

The polymerization of MMA is subject to various diffusional limitations: k_t, k_p and f decrease when monomer conversion χ increases. The associated phenomena are respectively known as the gel effect, the glass effect, and the cage effect. The glass effect is related to a decrease in the mobility of monomer molecules (hence a decrease in k_p) as χ increases. The cage effect is related to a reduction of the mobility of initiating radicals (hence a decrease in f) with increasing χ. Several approaches may be used to simulate the gel, glass and cage effects, i.e. to predict the dependence of k_t, k_p and f upon monomer conversion χ. In this work, three approaches are considered: an empirical, a semi-empirical and an analytical model. Their use within the thermochemical framework of Gayot and co-workers [7] is discussed and compared. The resulting modified thermochemical frameworks are referred to as the 'empirical', the 'semi-empirical' and the 'analytical' versions of the framework. Note that only an analytical approach was considered in the work of Gayot et al. [7].

TABLE I: FREE-RADICAL POLYMERIZATION MECHANISM [7].
(M: monomer, I: initiator, R•: macroradical, P: dead polymer, X: transfer agent, $C_{x:}$ transfer constant).

Step	**Equation**	**Kinetic coefficient**	**Reaction rate equation**
Initiator decomposition	$I_2 \rightarrow 2\ I\bullet$	k_d	$r_\mathrm{d} = 2fk_\mathrm{d}[I_2]$
Initiation	$I\bullet + M \rightarrow IM\bullet$	k_i	$r_\mathrm{i} = k_\mathrm{i}[I\bullet][M]$
Propagation	$R_n\bullet + M \rightarrow R_{n+1}\bullet$	k_p	$r_\mathrm{p} = k_\mathrm{p}[R\bullet][M]$
Termination by recombination by dismutation	$R_n\bullet + R_p\bullet \rightarrow P_{n+p+2}$ $R_n\bullet + R_p\bullet \rightarrow P_{n+1} + P_{p+1}$	k_t accounts for both termination mechanisms	$r_\mathrm{t} = k_\mathrm{t}[R\bullet]^2$ accounts for both termination mechanisms
Chain transfer reactions	$R_n\bullet + X \rightarrow P_n + X\bullet$	$k_{\mathrm{tr,X}}$	$r_{\mathrm{tr,X}} = C_\mathrm{X} k_\mathrm{p}[R\bullet][X]$

EMPIRICAL APPROACH

Hayden and Melville [20] measured the dependence of k_t and k_p as a function of monomer conversion χ during the isothermal polymerization of MMA at $T_0 = 22.5$ °C using azobisisobutyronitrile (AIBN) as an initiator. These measurements can be used to provide a simple phenomenological description of the auto-acceleration of the polymerization reaction. The cage effect is not considered (i.e. f is fixed) and the effect of chain transfer reactions is assumed to be negligible. The dependence of k_t and k_p upon χ at $T = T_0$ (= 22.5 °C) follows the fitted relations (see Fig. 2) [20]:

$$\ln k_t(T_0) = 11.21 - 13.52\chi \ , \tag{3}$$

and

$$\begin{cases} \ln k_p(T_0) = -1.15 & \text{for } 0 \le \chi < 0.5 \\ \ln k_p(T_0) = 6.82 - 16.44 & \text{for } 0.5 \le \chi \le 1 \end{cases} \tag{4}$$

respectively. In addition, we assume the values of k_t and k_p depend upon temperature via an Arrhenius law:

$$k_i(T) = k_i(T_0) \exp\left(-\frac{E_i}{R}\left(\frac{1}{T_0} - \frac{1}{T} \right) \right) , \tag{5}$$

where i is a subscript referring to termination or propagation, $k_i(T)$ is the value of the rate coefficient at temperature T, $k_i(T_0)$ is given via Eq. (3) or Eq. (4), E_i is the activation energy (for termination or propagation), and R is the ideal gas constant.

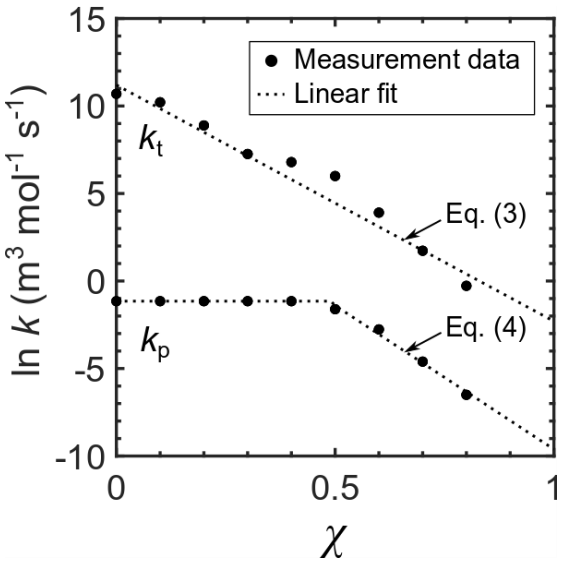

Figure 2: Dependence of k_t and k_p upon monomer conversion χ for the isothermal polymerization of MMA ($T_0 = 22.5$ °C) initiated by AIBN ($r_i = 8.36\times10^{-9}$ mol L^{-1} s^{-1}). Based on the measurement data from Hayden and Melville [20].

SEMI-EMPIRICAL APPROACH

We make use of the semi-empirical approach of Zoller [11] for the auto-acceleration of the polymerization reaction of MMA It combines the free volume-based calculation of k_p and f developed by Achilias [15–17] with an empirical model adapted from Russell [21] to describe k_t as a function of conversion χ at constant temperature T_0 (= 20 °C). The $\ln k_t(T_0)$ versus χ relation predicted with the semi-empirical model of Zoller [11] is shown in Fig. 3. The four successive regimes represent various phenomena leading to the decrease of the termination rate coefficient during the polymerization of MMA [11,16,21,22]. We make use of the Arrhenius correction given by Eq. (5) to account for the influence of temperature on the value of the kinetic rate coefficients [5]. Note that the effect of chain transfer reactions is assumed to be negligible.

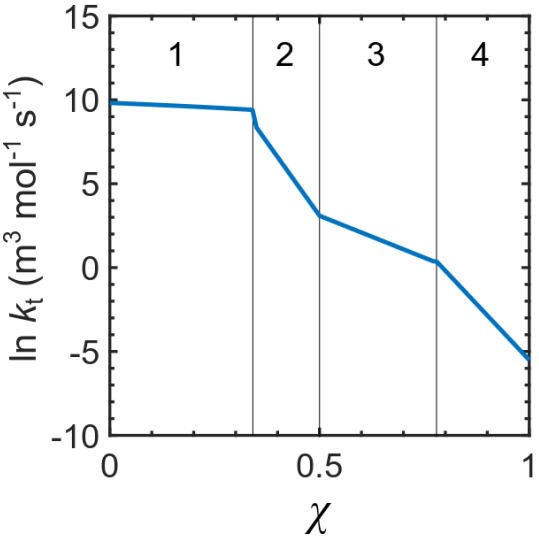

Figure 3: Dependence of k_t upon monomer conversion χ (at T_0 = 20 °C) based on the work of Zoller [11] and Russell [21]. Four conversion regimes are identified: (1) polymerization absent diffusional limitations, (2) start of the gel effect, (3) end of the gel effect (during which radical propagation slows down the decrease of k_t) and (4) the glass effect.

ANALYTICAL APPROACH

A modified version of the free volume-based analytical model of Achilias [7,15–17] is used to calculate the dependence of k_p, k_t, and f upon monomer conversion χ in the thermochemical framework of Gayot et al. [7]. An Arrhenius law is used to account for the dependence of temperature on the kinetic rate coefficients, and chain transfer reactions to monomer and initiator molecules are considered. Details for this analytical model are given in the work of Gayot et al. [7].

Numerical implementation of the thermochemical model

As detailed in the work by Gayot et al. [7], the thickness c_1 of the preform and the thickness c_2 of the infusion mold are discretized by Δy (= 1 mm). The processing time t_{tot} is discretized by Δt (= 7 s). Note that the value of t_{tot} includes the polymerization time of the resin and the cooling time of the plate. Convective boundary conditions are applied in order to match the measurement conditions applied by Gayot and co-workers [7]. In addition, the mold is assumed to consist of a homogenous plate of thickness c_2 = 15 mm made of a glass fiber reinforced polymer material with a thermal diffusivity α_2, and covered with a polymer-based heating film. A temperature T versus time t profile is imposed on the upper node of the mold to simulate external heating. For the other nodes corresponding to the mold, the temperature T is calculated as a function of time using a standard one-dimensional heat equation (i.e. Eq. (1) without an internal source term). The spatial discretization method and the set of boundary conditions described above are summarized in Fig. 4.

The MATLAB computing environment is used for the implementation of the three versions of the one-dimensional thermochemical model detailed above: the empirical, semi-empirical, and the analytical. The set of coupled equations is solved by making use of the semi-implicit Crank-Nicolson finite difference method [7,23]. The computation times for all predictions given in this paper do not exceed 60 s on a standard personal computer (equipped with an Intel® CoreTM i7-4600U 2.10GHz processor and with 16 Gb of RAM).

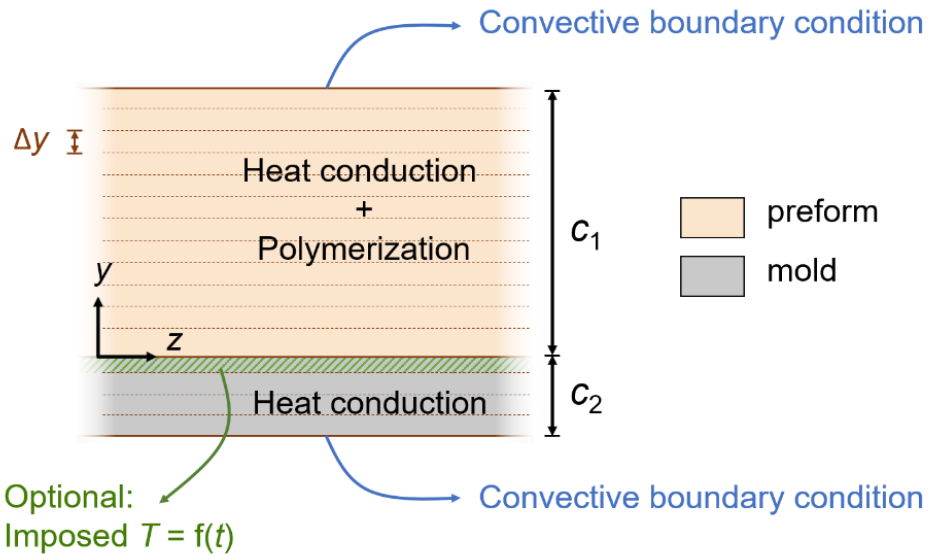

Figure 4: Boundary conditions used to solve the thermochemical problem. Preform thickness c_1 is equal to 73 mm and mold thickness c_2 is equal to 15 mm.

RESULTS AND DISCUSSION

The empirical, semi-analytical and analytical versions of the thermochemical models are calibrated by making use of the temperature profiles measured by Gayot and co-workers [7] during a single infusion test on a 73 mm-thick composite part referred to as 'plate B'. The processing parameters and measurement conditions for plate B are summarized in the Appendix [7]. Note that external heating was used to polymerize plate B, i.e. the temperature of the mold was controlled after infusion via a heating ramp from room temperature to 50 °C at a heating rate equal to 0.5 °C min^{-1}. For each version of the thermochemical model, a set of fitting parameters is adjusted in order to match the predicted T_t versus t curves with the measured ones for three measurement locations across the thickness of plate B. Details of the calibration method are given by Gayot et al [7]. The temperature profiles predicted with the three calibrated models are plotted along with the measured data for plate B in Fig. 5. In general, good agreement is observed between the model predictions (via the three versions) and the measurements. In particular, the dependence of peak shape, peak time and peak temperature upon measurement location across the thickness of the preform are reasonably well captured.

The analytical thermochemical model seems to offer the best prediction accuracy, see Fig. 5c. It relies on 9 adjusting parameters, i.e. more than the semi-empirical and empirical ones (which only have 7 and 4 adjusting parameters, respectively). This makes parameter identification slightly more challenging for the analytical model. However, the computing time remains below 60 s for all three frameworks. More importantly, the empirical model does not predict the correct shape for the temperature peaks (see Fig 5a). This may be attributed to the difference in experimental set-up between the present study and the measurements reported by Hayden and Melville [20]. On the other hand, the temperature profiles at the onset of the gel effect (close to t = 3

h) are not well captured by the semi-empirical model, see Fig 5b. This may be due to the imposed jump in the value of k_t at the boundary between conversion domains 1 and 2 (i.e. at χ = 0.35), see Fig. 3 [11]. Additionally, the empirical and semi-empirical models both introduce an artificial conversion breakpoint for the onset of the gel effect which may not be relevant with respect to the experimental conditions used by Gayot [7].

The predicted temperature profiles via the calibrated versions of the thermochemical model are now compared to the measurements reported by Gayot et al. for the production of a 73 mm-thick preform ('plate A' [7]).

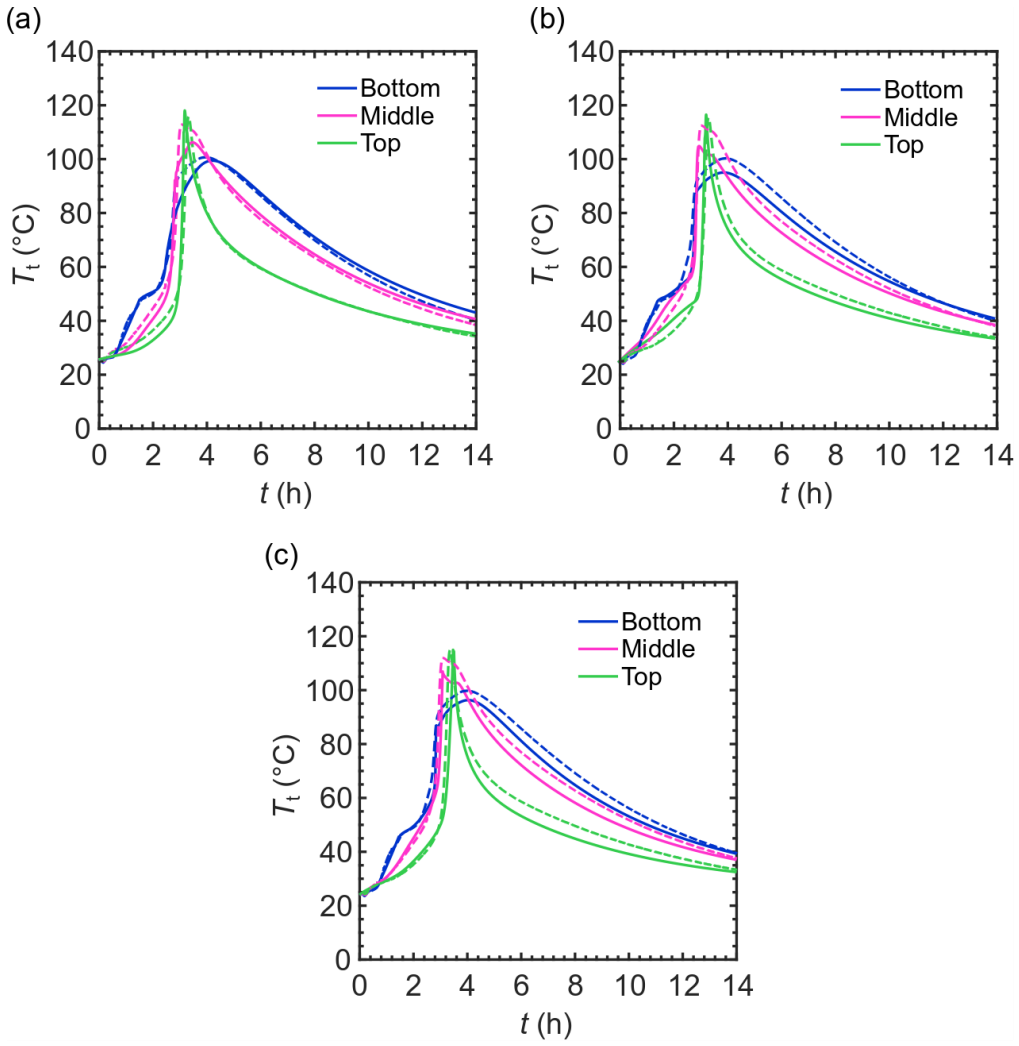

Figure 5: Model identification by making use of the measured temperature profiles for 'plate B' in the work of Gayot and co-workers [7]: measured (solid lines) and predicted (dashed lines) temperature T_t as a function of processing time t at different locations across the thickness of the plate (details of measurement locations are given in the Appendix). Predictions made via the (a) empirical version, (b) semi-empirical version and (c) analytical versions of the model of Gayot et al. [7].

The processing parameters and measurement conditions for plate A are summarized in the Appendix. Note that the only difference with plat B is that plate A is polymerized without external heating. The predicted and measured T_t versus t response at three measurement locations across the thickness of plate A is plotted in Fig. 6. The observed differences in the predictions of the three versions of the model with respect to the measurements are in the same line as those shown in Fig. 5 for plate B. The predicted peak times for plate A are in good agreement with the measured data. However, the empirical model fails at accurately capturing the peak shape and peak temperature (Fig. 6a), while the semi-empirical model struggles to give accurate predictions prior to the start of the gel effect (Fig. 6b). The analytical model gives the most accurate predictions of peak temperature and peak shape, while it also gives satisfactory agreement with the measurements at the onset of the gel effect, see Fig. 6c. This justifies the use of the analytical approach for the kinetic treatment of the gel effect in the thermochemical model of Gayot and co-workers [7].

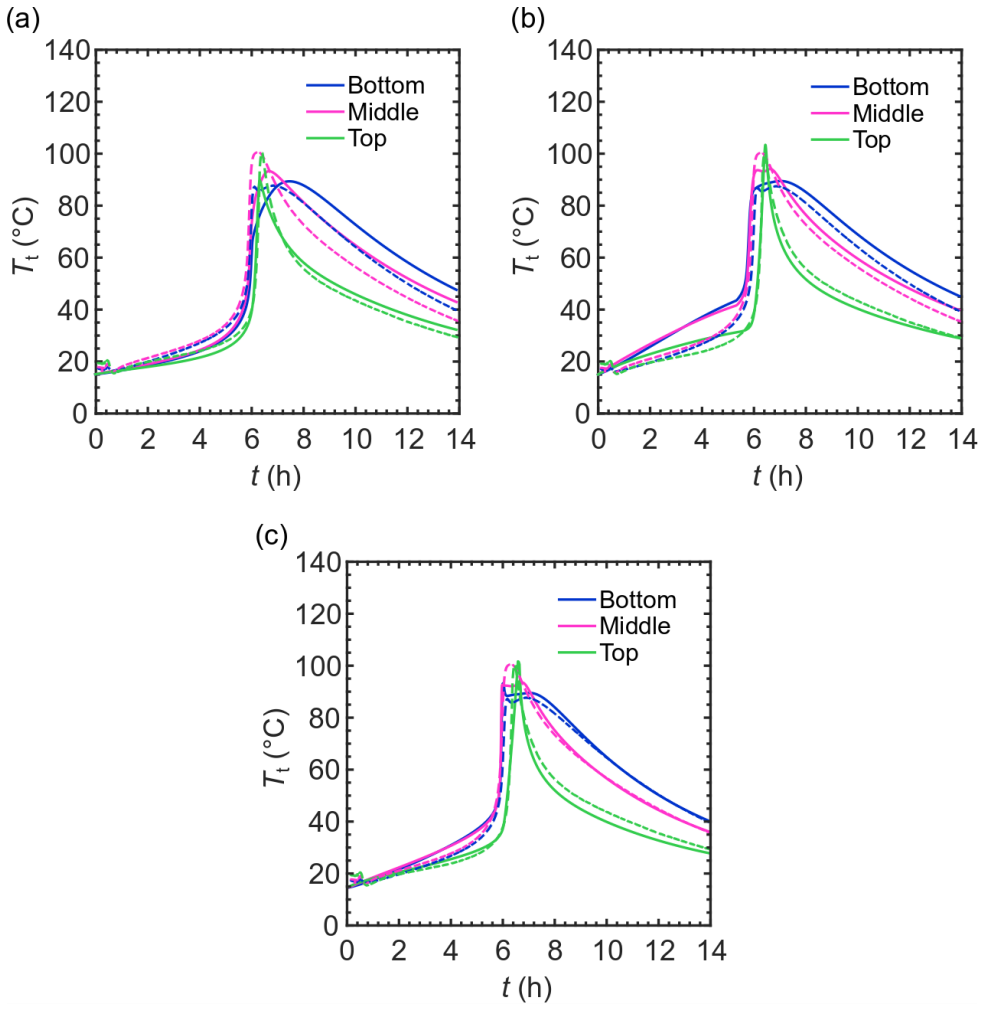

Figure 6: Predicted (solid curves) and measured (dashed curves) temperature T_t as a function of processing time t at different locations across the thickness of plate A: predictions via the (a) empirical, (b) semi-empirical and (c) analytical versions of the model of Gayot et al. [7]. Details of measurement locations are given in the Appendix.

Processing maps

We now make use of the calibrated thermochemical model of Gayot [7] with the analytical treatment for the gel effect to predict the maximum temperature T_{max} attained within the preform as a function of several processing parameters: mold set temperature T_p (Fig. 7a), mold heating rate $\dot{q}$ (Fig. 7b) and preform thickness c_1 (Fig. 7c). The material and processing parameters required for implementing the model are detailed in Tables 3 and 4 in the work of Gayot et al. [7]. The value of the ambient temperature T_{ext} is assumed to be equal to 25 °C for all simulations. Cavitation due to monomer boiling is assumed to occur when T_{max} exceeds the boiling temperature of the monomer under atmospheric pressure, i.e. T_b = 101 °C [7]. The processing regimes leading to $T_{max} > T_b$, i.e. where cavitation due to monomer boiling occurs, are shaded in blue.

The predicted T_{max} versus T_p data are plotted in Fig. 7a for several values of preform thickness c_1 and for a constant heating rate $\dot{q}$ = 0.5 °C min^{-1}. For the explored range of preform thicknesses, the value of T_{max} is found to be sensitive to the setpoint temperature of the mold in the regime 30 °C < T_p < 70 °C. When the value of T_p lies within this range, T_{max} increases significantly with increasing mold set temperature.

Next, the predicted value for T_{max} is plotted in Fig. 7b as a function of mold heating rate $\dot{q}$ for selected values of preform thickness and T_p = 50 °C. The value of T_{max} only increases significantly with increasing heating rate within a relatively narrow range for $\dot{q}$ (0.1 °C min^{-1} < $\dot{q}$ <0.5 °C min^{-1}).

Finally, the influence of preform thickness c_1 upon T_{max} is explored. The predicted value of T_{max} is plotted as a function of c_1 in Fig. 7c with external heating (T_p = 50 °C and $\dot{q} = 0.5$ °C min^{-1}) and without external heating ($\dot{q} = 0$). In both cases, the value of T_{max} increases monotonically with increasing preform thickness for c_1 < 8 cm, and becomes insensitive to the selected value of preform thickness for c_1 close to or above 8 cm. Note that the processing window requiring T_{max} < 101 °C shrinks as preform thickness increases (see Fig. 7a and 7b).

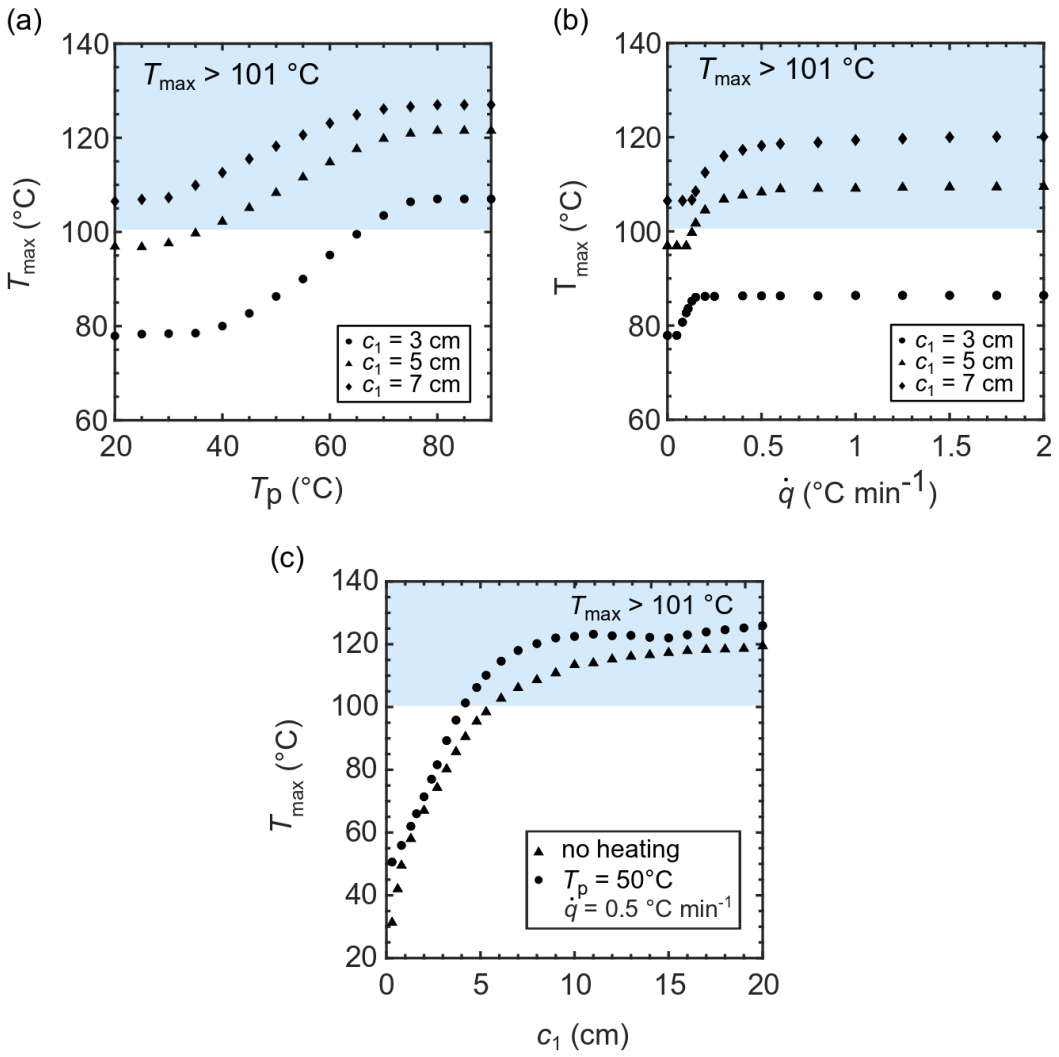

Figure 7: Predicted maximum temperature across the thickness of the preform during polymerization, T_{max}, as a function of (a) mold set temperature T_p for selected values of preform thickness c_1 ($\dot{q}$ = 0.5 °C min^{-1}), (b) heating rate $\dot{q}$ for selected values of preform thickness c_1 (T_p = 50 °C) and (c) preform thickness c_1 with heating (T_p = 50 °C, $\dot{q}$ = 0.5 °C min-1) and without heating.

Processing maps can be used to identify the optimum combinations of preform thickness and mold heating parameters, i.e. those leading to short processing times without inducing monomer boiling and consecutive void nucleation and growth. Two examples of such maps are presented in Fig. 8. The first map is constructed with axes $\dot{q}$ and T_p and shown in Fig. 8a [7]. The boundary corresponding to T_{max} =101 °C is plotted for several values of preform thickness c_1. For each value of c_1, this boundary divides the map into two regimes: a T_{max} < 101 °C processing window where monomer boiling does not occur, and a T_{max} ≥ 101 °C window where boiling (and cavitation) is expected to occur. The second processing map is constructed with axes c_1 and T_p, see Fig. 8b. The T_{max} =101 °C boundary is now plotted for selected values of heating rate $\dot{q}$. Processing windows leading to cavitation are identified in Fig. 8 as blue-shaded areas for the case where c_1 is constant and set equal to 4 cm (Fig. 8a) and for the case where $\dot{q}$ is constant and set equal to 0.2 °C min^{-1} (Fig. 8b).

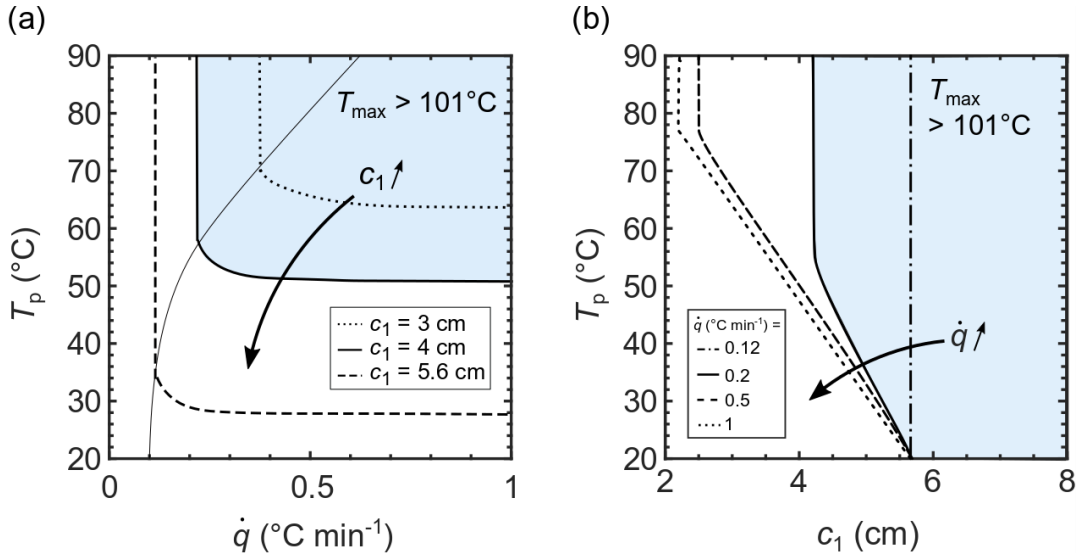

Figure 8: Processing maps for the in-situ polymerization of an MMA-infused thick glass fiber preform: (a) mold set temperature T_p as a function of heating rate $\dot{q}$ with predicted T_{max} = 101 °C boundaries for selected values of heating rate (T_{ext} = 25 °C) and (b) mold set temperature T_p as a function of preform thickness c_1 with predicted T_{max} = 101 °C boundaries for selected values of heating rate $\dot{q}$ (T_{ext} = 25 °C).

CONCLUSIONS

We have re-examined the kinetic treatment for the gel effect in the recent thermochemical model of Gayot et al. [7] to predict the maximum temperature (and the occurrence of monomer boiling) during the polymerization of an MMA-infused fibrous preform. Three approaches to describe the auto-acceleration of the MMA polymerization reaction have been considered: an empirical approach, a semi-empirical approach, and an analytical model. When calibrated, the three versions of the thermochemical framework lead to good agreement between predictions and measured data from infusion tests, with no significant difference in computational cost. However, the analytical treatment was found to give the most accurate predictions for the temperature profiles over the entire polymerization time. In particular, peak shape, peak time and peak temperature are very well captured for two different mold heating conditions. This justifies the choice for the analytical approach for the kinetic treatment within the thermochemical framework of Gayot and co-workers.

REFERENCES

[1] Cousins, D. S., 2018, "Advanced Thermoplastic Composites for Wind Turbine Blade Manufacturing," Colorado School of Mines.

[2] Trommsdorff, V. E., Köhle, H., and Lagally, P., 1948, "Zur polymerisation des methacrylsäuremethylesters," *Die Makromolekulare Chemie*, **1**(3), pp. 169–198.

[3] Norrish, R. G. W., and Smith, R. R., 1942, "Catalyzed Polymerization of Methyl Methacrylate in the Liquid Phase," *Nature*, **150**, pp. 336–337.

[4] Charlier, Q., 2015, "Adhesion Phenomena in Thermoplastic Composites Based on Acrylic Matrices Obtained by Free Radical Polymerization," Institut National des Sciences Appliquées de Lyon.
[5] Suzuki, Y., Cousins, D. S., Wassgren, J., Kappes, B. B., Dorgan, J., and Stebner, A. P., 2018, "Kinetics and Temperature Evolution during the Bulk Polymerization of Methyl Methacrylate for Vacuum-Assisted Resin Transfer Molding," *Compos. Part A Appl. Sci. Manuf.*, **104**, pp. 60–67.
[6] Borzacchiello, A., Ambrosio, L., Nicolais, L., Harper, E. J., Tanner, K. E., and Bonfield, W., 1998, "Isothermal and Non-Isothermal Polymerization of a New Bone Cement," *J. Mater. Sci. Mater. Med*, **9**, pp. 317–324.
[7] Gayot, S. F., Bailly, C., Pardoen, T., Gérard, P., and Van Loock, F., 2020, "Processing Maps from Thermochemical Modelling of In-Situ Polymerization of Thick Fiber-Reinforced Methacrylic Composites," submitted for publication.
[8] Hui, A. W., and Hamielec, A. E., 1972, "Thermal Polymerization of Styrene at High Conversions and Temperatures. An Experimental Study," *J. Appl. Polym. Sci.*, **16**(3), pp. 749–769.
[9] Tefera, N., Weickert, G., and Westerterp, K. R., 1997, "Modeling of Free Radical Polymerization up to High Conversion. II. Development of a Mathematical Model," *J. Appl. Polym. Sci.*, **63**(12), pp. 1663–1680.
[10] Sangwai, J. S., Bhat, S. A., Gupta, S., Saraf, D. N., and Gupta, S. K., 2005, "Bulk Free Radical Polymerizations of Methyl Methacrylate under Non-Isothermal Conditions and with Intermediate Addition of Initiator: Experiments and Modeling," *Polymer*, **46**(25), pp. 11451–11462.
[11] Zoller, A., Gigmes, D., and Guillaneuf, Y., 2015, "Simulation of Radical Polymerization of Methyl Methacrylate at Room Temperature Using a Tertiary Amine/BPO Initiating System," *Polym Chem*, **6**(31), pp. 5719–5727.
[12] Marten, F. L., and Hamielec, A. E., 1979, "High Conversion Diffusion-Controlled Polymerization," *Polymerization Reactors and Processes, ACS Symposium Series*, J.N. Henderson, ed., American Chemical Society, Washington, DC (USA), pp. 43–70.
[13] Hamielec, A. E., 1983, "Recent Developments in Free-Radical Polymerization at High Conversion - Diffusion-Controlled Termination and Propagation," *Chem Eng Commun*, **24**(1–3), pp. 1–19.
[14] Zhu, S., and Hamielec, A. E., 1989, "Chain-Length-Dependent Termination for Free Radical Polymerization," *Macromolecules*, **22**(7), pp. 3093–3098.
[15] Achilias, D., and Kiparissides, C., 1988, "Modeling of Diffusion-Controlled Free-Radical Polymerization Reactions," *J. Appl. Polym. Sci.*, **35**(5), pp. 1303–1323.
[16] Achilias, D. S., and Kiparissides, C., 1992, "Development of a General Mathematical Framework for Modeling Diffusion-Controlled Free-Radical Polymerization Reactions," *Macromolecules*, **25**(14), pp. 3739–3750.
[17] Achilias, D. S., and Sideridou, I. D., 2004, "Kinetics of the Benzoyl Peroxide/Amine Initiated Free-Radical Polymerization of Dental Dimethacrylate Monomers: Experimental Studies and Mathematical Modeling for TEGDMA and Bis-EMA," *Macromolecules*, **37**(11), pp. 4254–4265.
[18] Buback, M., Egorov, M., Gilbert, R. G., Kaminsky, V., Olaj, O. F., Russell, G. T., Vana, P., and Zifferer, G., 2002, "Critically Evaluated Termination Rate Coefficients for Free-Radical Polymerization, 1," *Macromolecular Chemistry and Physics*, **203**(18), pp. 2570–2582.
[19] Dotson, N. A., Galvan, R., Laurence, R. L., and Tirrell, M., 1996, *Polymerization Process Modeling*, VCH Publishers, Inc., New York, NY (USA).
[20] Hayden, P., and Melville, H., 1960, "The Kinetics of the Polymerization of Methyl Methacrylate. I. The Bulk Reaction," *J Polym Sci*, **43**(141), pp. 201–214.
[21] Russell, G. T., Napper, D. H., and Gilbert, R. G., 1988, "Termination in Free-Radical Polymerizing Systems at High Conversion," *Macromolecules*, **21**(7), pp. 2133–2140.
[22] Zhu, S., Tian, Y., Hamielec, A. E., and Eaton, D. R., 1990, "Radical Concentrations in Free Radical Copolymerization of MMA/EGDMA," *Polymer*, **31**(1), pp. 154–159.
[23] Crank, J., and Nicolson, P., 1947, "A Practical Method for Numerical Evaluation of Solutions of Partial Differential Equations of the Heat-Conduction Type," *Mathematical Proceedings of the Cambridge Philosophical Society*, **43**(1), pp. 50–67.

APPENDIX: PROCESSING CONDITIONS OF PLATES A AND B (based on the work of Gayot et al. [7])

Materials

Composite preforms were made from quasi-unidimensional non-crimp glass fabric plies (Chomarat, France) with an areal weight of 1.03 kg m^{-2} (85% warp and 15% weft). The resin system comprised an infusion-grade monomer (Elium® 191OSA of Arkema, France) and a peroxide initiator (Luperox® K10 of Arkema, France). The consumables for bagging and infusion were obtained from Diatex SAS (France). Thermocouples of type J (TC S.A., France) were used to measure the temperature within the composite preforms during the infusion experiments.

Composite Production

Composite plates were processed via vacuum infusion of glass fiber-based preforms using the setup illustrated in Fig. 9. The manufacturing conditions leading to plates A and B are detailed in Table II: different mold set temperature values were used. Upon completion of the polymerization reaction, each plate was left to cool down to room temperature and released from the mold. Final fiber volume fractions were close to 0.5.

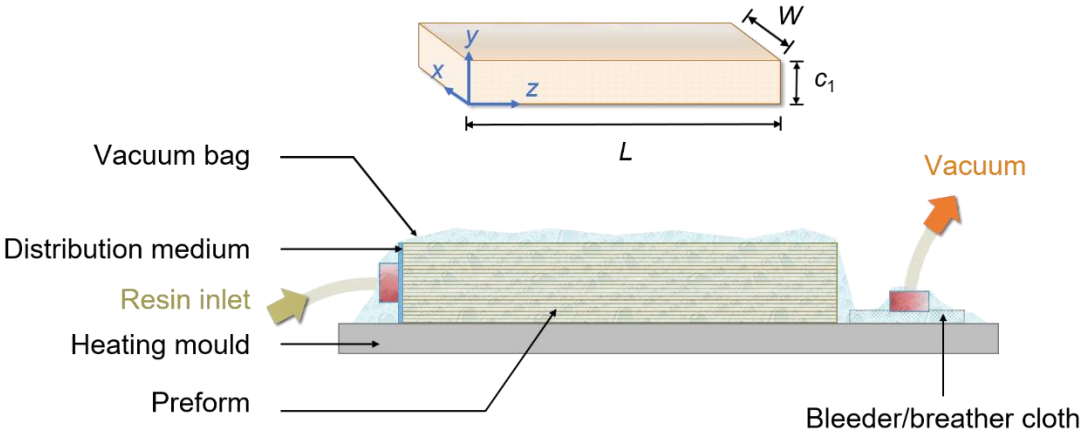

Figure 9: Experimental setup used by Gayot et al. [7] for the vacuum infusion of composite plates of variable thickness c_1 (L = 60 cm, W = 40 cm).

TABLE II: MANUFACTURING CONDITIONS FOR PLATES A AND B (from Gayot et al. [7])

Set of experimental conditions	**A**	**B**
Ambient temperature during experiment	17 °C	25 °C
Laminate structure	90 plies, $(AB)_{45}/(BA)_{45}$	
Final part thickness	c_1 = 73 mm	
Location of thermocouples	Bottom : ply 5/90 ($y \approx 0.06c_1$) Middle : ply 45/90 ($y = 0.50c_1$) Top : ply 85/90 ($y \approx 0.94c_1$)	
Preparation and infusion of resin mix	Combination of resin with 3 phr initiator, 5-min mechanical stirring, 1-min degassing at 100 mbar, infusion in the *z*-direction at 100 mbar and room temperature, clamping of resin and vacuum tubes	
Temperature program applied to mold after infusion	No heating	Heating to 50 °C (0.5 °C/min), 30-min plateau at 50 °C, heating switched off